Geomechanics and Engineering, *Vol. 40, No. 46 (2025) 251-262*
https://doi.org/10.12989/gae.2025.40.4.251

The enhanced bishop method for considering effective stress in unsaturated soils

Weiliang Ma[1a] and Longtan Shao*[2]

[1]*School of Mechanics and Aerospace Engineering, Dalian University of Technology, Dalian, Liaoning, China*
[2]*State Key Laboratory of Structural Analysis, Optimization and CAE Software for Industrial Equipment, Dalian University of Technology, Dalian Liaoning, China*

(*Received October 23, 2024, Revised February 1, 2025, Accepted February 10, 2025*)

Abstract. At present, the widely used bishop stability analysis method does not consider the unsaturated effective stress, and the effective stress theory is unclear. To address these questions, this study initially explores a novel methodology for determining pore water pressure via the phreatic line. Subsequently, this study integrates the unified effective stress equation for both saturated and unsaturated soils, known for its clear physical significance, to propose an enhanced Bishop method(EBM) that accounts for effective stress in unsaturated soils. This EBM features a comprehensive theoretical framework, enabling direct stability analysis based on the phreatic line and demonstrating significant value for engineering applications. The reliability of the computational procedure of the EBM is validated through a saturated slope case study. Building upon this validation, the study further investigates the impact of incorporating unsaturated effective stress on slope stability. The results show that the deeper most dangerous sliding surface corresponds to an increase in the factor of safety(FOS) from 1.01% to 20.51% when considering the unsaturated effective stress. Overall, the integration of unsaturated effective stress exerts a positive influence on slope stability, underscoring the significance of this method for stability analysis and engineering design applications.

Keywords: bishop method; phreatic line; stability; unified effective stress equation; unsaturated soil

1. Introduction

Properly characterizing the stress state of soil is a fundamental prerequisite for investigating soil deformation and strength (Fredlund *et al*. 1978, Fredlund 2006, Skempton 1960, 1961). Determining the shear strength and deformation of soil layers using effective stress principles is grounded in robust theoretical foundations and holds significant implications for the stability assessment of geotechnical engineering(De Boer and Ehlers 1990, Gudehus 2021, Li *et al.* 2023, Xu *et al*. 2021, Yates and Russell 2023). However, accurately determining the effective stresses in unsaturated soils and the strength of the soil has long been a major challenge in geotechnical engineering. In 1959, Bishop (1959) extended Terzaghi's effective stress theory for saturated soils to encompass unsaturated soils, proposing a corresponding effective stress expression. Nevertheless, the application of Bishop's effective stress expression to unsaturated soils exhibits limitations, garnering widespread attention(Bishop and Blight 1963, Jennings and Burland 1962, Khalili and Khabbaz 1998, Khalili *et al.* 2004). Assuming that the effective stress coefficient χ equates to the degree of saturation frequently results in substantial prediction errors. Recent investigations into the microstructure of soils have revealed that immobile water, adhering to soil particles via physicochemical bonds, resides in micropores, whereas free water, primarily governed by capillary effects, occupies relatively larger pores. Building on this understanding, Lu *et al*. (2010) proposed utilizing effective saturation as a suitable substitute for the effective stress parameter. In 1996, Longtan Shao (Shao *et al*. 2014a, b) separately considered the effects of external load and pore fluid pressure, treating the soil skeleton and pore fluid as distinct entities, and derived their respective equilibrium equations. By comparing with the total stress equation, he derived Terzaghi's effective stress expression, elucidating the physical meaning of effective stress: the stress on the soil skeleton generated by external forces, excluding pore fluid pressure. In 1999, he employed the same methodology to derive the effective stress expression for unsaturated soils (Shao *et al.* 2018a, b), thereby establishing a unified effective stress equation for both saturated and unsaturated soils.

Slope stability analysis, a crucial concern in the natural environment and engineering geology, has been extensively researched (Hu *et al*. 2021, Shin 2023, Tran *et al.* 2023). Matric suction influences the effective stress in unsaturated soils, which in turn governs the soil's shear strength properties, making it a critical factor (Cheng *et al*. 2024, Deng *et al.* 2019, Zhai *et al.* 2022). The majority of documented slope failures occur in unsaturated zones within the slope, and variations in unsaturated conditions adversely affect slope stability (Garakani *et al*. 2020, Lu *et al.* 2013, Oh and Lu 2015, Sivakumar Babu and Murthy

*Corresponding author, Professor
E-mail: shaolt2022@163.com
[a]Ph.D. Student
E-mail: maweiliang828@163.com

ISSN: 2005-307X (Print), 2092-6219 (Online)

2005, Song *et al.* 2016, Xu *et al*. 2021, Xu and Yang 2018, Zhang *et al*. 2013, 2015, Zhai *et al*. 2022). Hence, acknowledging the significant role of matric suction or soil saturation in geotechnical design (Alencar *et al*. 2021, Pirjalili *et al.* 2020), and incorporating these theoretical complexities into analysis, can render slope design more robust and reliable.

Presently, stability analysis predominantly encompasses limit equilibrium methods (LEM) (Bishop 1955, Morgenstern and Price 1965, Shin 2023), finite element methods (FEM) (Tran *et al*. 2023, Cheng *et al*. 2007, Hua *et al.* 2022), and finite element limit equilibrium methods (FELEM) (Liu *et al*. 2015). Among these, LEM is the most extensively utilized in engineering practice, primarily involving the analysis of the static equilibrium of unstable soil masses and assessing slope stability based on the Mohr-Coulomb strength criterion. The Bishop method (Bishop 1955) is the most prevalent within LEM. Traditional Bishop methods (TBM) presuppose that the pore water pressure on the slip surface is either zero or positive, thereby overlooking the effect of matric suction when the sliding surface lies within the unsaturated zone. Although some researchers have endeavored to incorporate the effect of matric suction into TBM, there remains a lack of systematic theoretical analysis and discussion concerning the calculation and implementation of unsaturated effective stress in the Bishop method. In general, the widely used bishop stability analysis method has the following problems: (1)it overlooks the effective stress in unsaturated zones, (2)relies on an incomplete effective stress theory, (3)lacks a robust theoretical foundation for strength conditions in stability assessments, and (4)suffers from ambiguous methodologies and inaccuracies in calculating pore water pressure.

In light of this, this paper proposes an EBM that accounts for the effective stress in unsaturated soils. This method employs a unified effective stress equation with clear physical significance for both saturated and unsaturated soils, along with their shear strength theory. The pore water pressure is approximated directly based on the phreatic line. This method is computationally simple and theoretically robust, enabling direct slope stability analysis based on the phreatic line. It holds substantial engineering application value and is of considerable importance for stability analysis and design in engineering.

2. Method for calculating approximate pore pressure and effective stress of soil

2.1 Unified calculation method of pore water pressure in saturated and unsaturated soils

In the stability analysis of geotechnical engineering projects, water significantly impacts the stability of geotechnical structures in addition to soil properties and geometric parameters. The primary reason is that pore water pressure affects the soil's effective stress, thereby influencing its shear strength. Directly calculating the pore water pressure in the soil layer from the phreatic line and subsequently determining the effective stress would offer a quick and straightforward method. This approach would enhance the Bishop method by incorporating unsaturated effective stress.

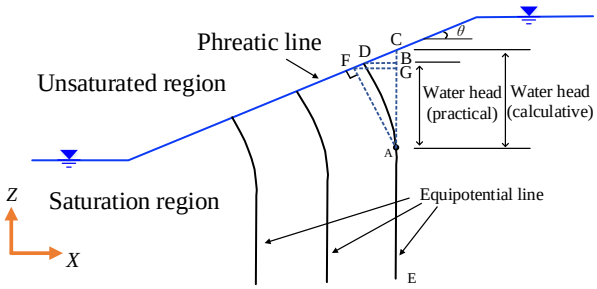

Fig. 1 Diagram of head loss caused by penetration velocity in saturated region

The pore water pressure in both the saturated and unsaturated zones is approximately determined based on the phreatic line. The fundamental assumptions are: (1) ignoring head loss due to seepage velocity; (2) disregarding the impact of soil volume deformation on seepage; (3) assuming the matric suction of pore water in the unsaturated zone adheres to the soil water characteristic curve. The phreatic line (free water surface) delineates the soil layer into saturated and unsaturated zones, with the area above the phreatic line being the unsaturated zone and the area below being the saturated zone. Therefore, the total hydraulic head of the pore water, irrespective of whether it is in the saturated or unsaturated zone, is

$$H = z + \frac{u_w}{\rho_w g} \tag{1}$$

where H is the hydraulic head, z is the position head, $\frac{u_w}{\rho_w g}$ is the pressure head, ρ_w is the water density, and g is the gravitational acceleration.

At every point along the phreatic line, the pore water pressure is zero. Using the phreatic line as the reference plane and assuming that the pore water pressure follows a hydrostatic distribution, it can be expressed as

$$u_w = -\rho_w g\left(z - z_0\right) \tag{2}$$

where z_0 is the vertical coordinate of the phreatic line corresponding to the same horizontal coordinate as the calculation point. Eq. (2) represents the unified pore water pressure equation for both saturated and unsaturated soils.

2.2 Error analysis of pore pressure calculation results based on phreatic line

Substituting a point of hydrostatic pressure for the actual pore water pressure is equivalent to assuming that the pore water is at rest equilibrium. This also means that the head loss caused by the seepage velocity is ignored. The head loss caused by seepage velocity can be evaluated by using the flow-net method. Take the saturation region as an

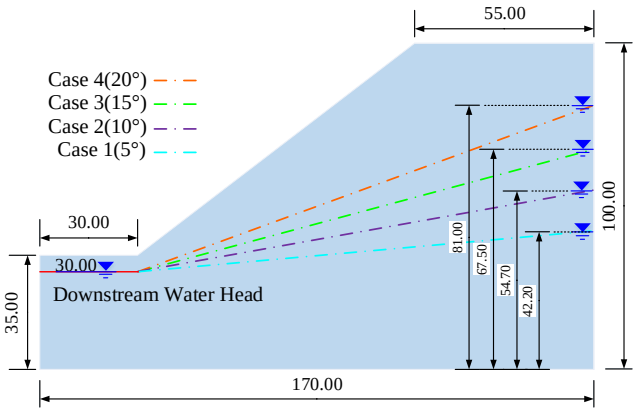

Fig. 2 Calculation model of pore water pressure based on phreatic line

example, as shown in Fig. 1, where the isopotential lines are perpendicular to the phreatic lines, and each point on each equipotential line has the same total water head (water potential). Suppose that the equipotential line through point A is EAD, the vertical line through point A intersects the phreatic line at point C with the vertical coordinate marking z_0^A, and the horizontal line through point D (the intersection of the equipotential line and the phreatic line) intersects the line segment AC at B. Then the actual pressure at point A is $\rho_w g(z_B - z_A)$, and the pressure calculated from the hydrostatic pressure is $\rho_w g(z_0^A - z_A)$, resulting in an error of $\rho_w g(z_0^A - z_B)$.

Perpendicular to the seepage line through point A, intersecting with the phreatic line at point F. Then, the equipotential line (AD segment) above point A must be located on the right side of the vertical line, and the CG segment is the maximum head loss at point A. Therefore, the maximum relative head loss at each point can be expressed as

$$\eta = \frac{z_0 - z'}{z_0 - z} = \sin^2\theta \tag{3}$$

where z' is the vertical coordinate of the sought position perpendicular to the saturation line in the vertical profile; θ is the angle between the saturation line and the horizontal plane. Therefore, the maximum error in pressure calculated according to hydrostatic pressure is $\rho_w g(z_0 - z)\sin^2\theta$.

When the angle between the saturation line and the horizontal direction is less than 20º, the discrepancy between the head calculation results and the flow net equipotential lines is under 10%, signifying that the flatter the saturation line, the smaller the error. Thus, if the precision requirement is not stringent, the head loss due to seepage velocity can be disregarded, and hydrostatic pressure can be used to approximate the pore water pressure.

In order to deeply investigate the pore water pressure calculation error based on the phreatic line, the dam body shown in Fig. 2 was selected as the research object in this study, and four different upstream and downstream head boundary conditions were set, corresponding to the seepage line inclination angles of 5º, 10º, 15º and 20º, respectively. Under these boundary conditions, the saturated seepage was

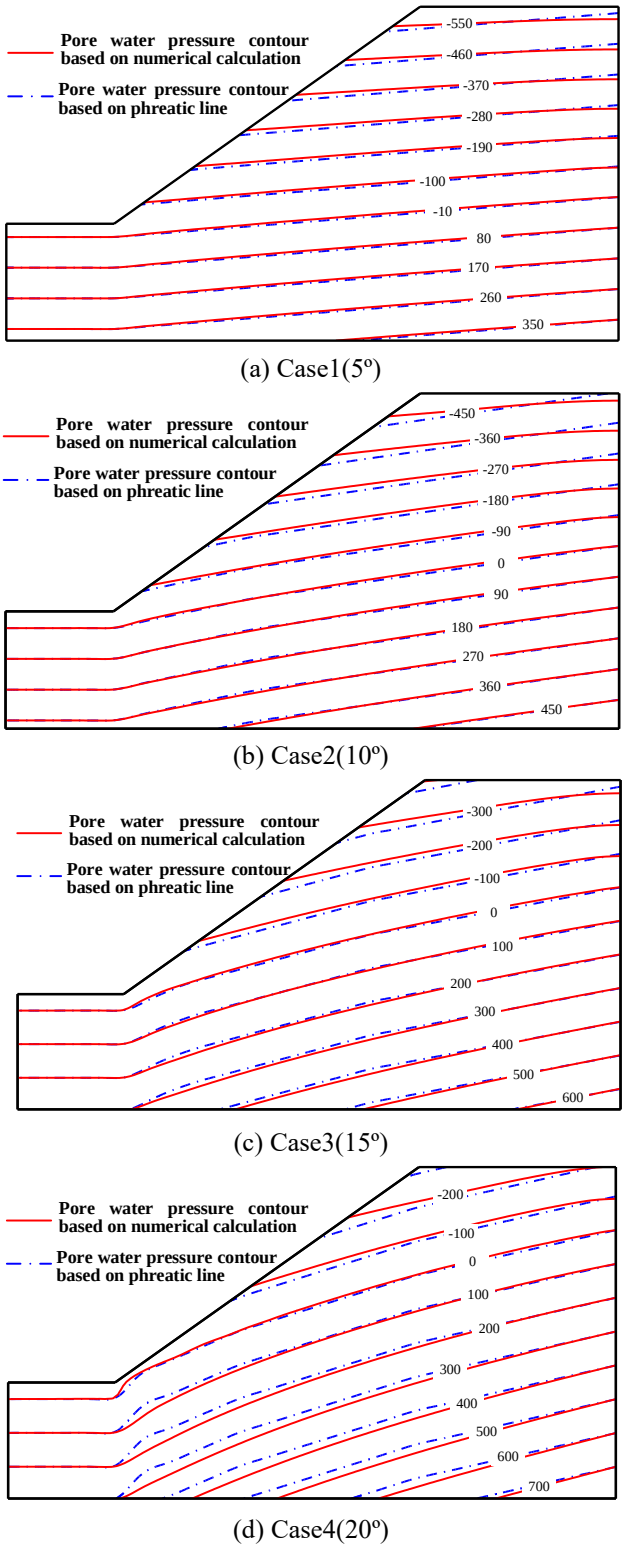

Fig. 3 Pore water pressure contour(kPa)

numerically analyzed using the FEM, and the pore water pressure field was calculated for the four cases. Meanwhile, based on the location of the phreatic line determined by the numerical analysis, the pore water pressure field of the dam body under the four different head boundary conditions was calculated by using Eq. (2). The accuracy of the pore water pressure calculation method based on the phreatic line is

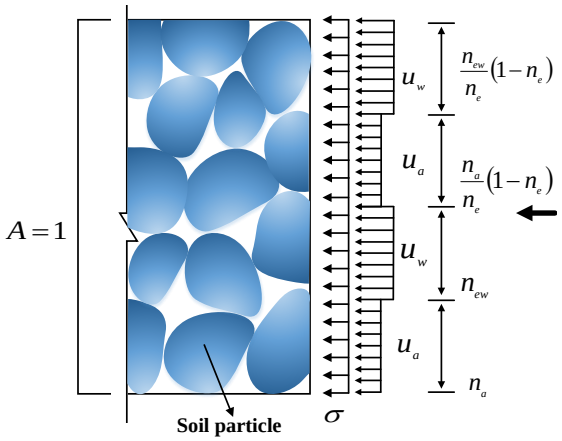

Fig. 4 Internal Force Diagram for an Arbitrary Cross-Section of Soil

evaluated by comparing the results of the pore water pressure field obtained from these two calculation methods.

In order to carry out an accurate comparison of the pore water pressure calculation results of the two methods, the method of plotting the results of the pore water pressure field calculation based on the seepage line on the same contour map as that based on the numerical analysis method. As shown in Fig. 3, through the comparative analysis, it can be observed that at the location of the downstream horizontal phreatic line, the pore water pressure contours obtained by the two calculation methods are identical. However, in the slope region, the deviation between the pore water pressure contours obtained by the two calculation methods increases with the increase of the average dip angle of the phreatic line. Specifically, under the conditions of 5º, 10º and 15º, the deviation between the pore water pressure contours obtained by the two methods is relatively small, and the contours of the two methods coincide in most areas. At an inclination of the phreatic line of 20º, the deviation of the pore water pressure contours obtained by the two methods is slightly larger, but the average error is only within 10%.

This phenomenon indicates that when the dip angle of the phreatic line is less than 20º, the pore water pressure calculation method based on the phreatic line has a small error, and its calculation accuracy is sufficient to meet the needs of engineering practice.

2.3 Unified effective stress equation for both saturated and unsaturated soils

Longtan Shao applies the theory of continuous medium mechanics to derive a unified effective stress formula for saturated and unsaturated soil by considering the effects of external load and pore fluid pressure separatel (Shao et al. 2013, 2014a, b, 2015, 2018a, b, c). It is illustrated that the effective stress, intergranular stress and soil skeleton stress can be consistent, i.e., the intergranular stress and soil skeleton stress that do not include the action of pore water pressure are the effective stress. The derivation process of the effective stress equation for saturated and unsaturated soils unified is briefly explained in the following.

By separately considering the pore fluid pressure and other external forces at any point on a soil cross-section, the relational expressions between total stress, external force-induced soil skeleton stress, and pore fluid pressure can be derived, namely the effective stress equation. It reveals that the effective stress equation fundamentally describes the relationship between the internal forces at a specific point in the soil.

As depicted in Fig. 4, the total normal internal force is the sum of the soil skeleton internal force induced by external forces, the internal force resulting from pore fluid pressure acting on the soil skeleton, and the internal force resulting from pore fluid pressure acting on the pore area, i.e.

$$N_t = N^s + N_f^s + N_f^v \tag{4}$$

where N_t is the total normal internal force on the soil cross-section, N^s is the normal internal force generated by external forces acting on the skeleton excluding pore fluid pressure, N_f^s is the normal internal force generated by pore fluid (both pore water and pore gas) pressure acting on the skeleton, and signifies the normal internal force generated by pore fluid pressure acting on the pore area. Eq. (5) is obtained according to Fig. 4.

$$\begin{cases} N^s = \sigma A \\ N_f^s = u_w \dfrac{n_{ew}}{n_e}(1-n_e)A + u_a \dfrac{n_a}{n_e}(1-n_e)A \\ N_f^v = u_w \dfrac{n_{ew}}{n_e} n_e A + u_a \dfrac{n_a}{n_e} n_e A \end{cases} \tag{5}$$

where n_e is the effective porosity (considering pore water closely bonded with soil skeleton particles and jointly bearing and transmitting the load as part of the skeleton, the ratio of pore volume to total volume is defined as the effective porosity); n_{ew} is the effective porosity corresponding to pore water; n_a is the porosity corresponding to pore gas; and A is the total area of the soil cross-section.

Among these, $\frac{n_{ew}}{n_e} = S_e$ represents the effective degree of saturation of the soil. By substituting Eq. (5) into Eq. (4) and rearranging, we obtain

$$\sigma = \sigma_t - u_a + S_e(u_a - u_w) \tag{6}$$

Eq. (6) represents the effective stress expression for unsaturated soils, which is also applicable to saturated soils. When S_e=1, Terzaghi's effective stress equation is obtained. For saturated soils, the degree of saturation is 1 and the matrix suction is zero, and the same can be shown that the effective stress of saturated soils is a specific condition for the effective stress of unsaturated soils. That is, Eq. (6) is the unified effective stress equation for saturated and unsaturated soils. The effective stresses in saturated and unsaturated soils have the same physical meaning, i.e., the external soil skeleton stresses without considering the pore fluid action. Here, S_e is the effective degree of saturation of

the pore water considered as part of the soil skeleton.

$$S_e = (S - S_r)/(1 - S_r) \tag{7}$$

where S is the saturation corresponding to the absolute water content, and S_r=n_r/n represents the residual saturation (n_r denotes the residual porosity).

In geotechnical engineering, the total stress of the soil is relatively easy to obtain. According to the above pore water pressure calculation equation based on the phreatic line, the pore water pressure can be easily obtained. Moreover, in open formations, the pore gas pressure (u_a) is generally considered to be 0. Therefore, using Eq. (6), the effective stress of the soil can be easily obtained.

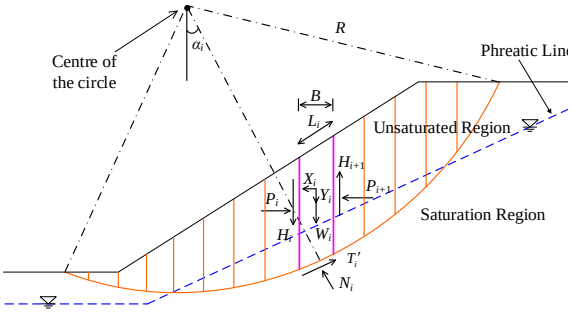

Fig. 5 Diagram of the Forces in the EBM

3. Conditions for shear strength in stability analysis

The strength and deformation of soil correspond to those of the soil skeleton, which are governed by the stress within the skeleton. This stress comprises two components: (i) stress induced by all external forces excluding pore water pressure, and (ii) stress induced by pore water pressure. These components are termed external soil skeleton stress(ESSS) and pore pressure soil skeleton stress(PPSSS), respectively. According to the unified effective stress equation discussed earlier, Terzaghi's effective stress represents the stress in the soil skeleton resulting from all external forces excluding pore water pressure, hence, ESSS equates to effective stress. Both stress types influence the shear strength and volumetric deformation of the soil, albeit differently. The strength of the soil skeleton encompasses shear strength due to external soil skeleton stress and shear strength due to pore fluid pressure. The Bishop method employs the Mohr-Coulomb strength criterion. For instance, considering the shear strength of the soil skeleton in unsaturated soil, it is expressed as

$$\tau_f = c' + \left\{\sigma_t - (1 - \frac{a_c \tan\psi}{\tan\varphi'})[u_a - S_e(u_a - u_w)]\right\}\tan\varphi' \tag{8}$$

where a_c is the contact area coefficient between skeleton particles, and tanψ is the shear strength parameter of the contact surface between soil particles. When S_e = 1, Eq. (8) depicts the shear strength of the soil skeleton in saturated soil, with the expression for shear strength aligning with that proposed by Skempton (1961).

Pore water pressure contributes to the shear strength of soil only when it induces contact forces between particles. Given that the contact area between soil particles is typically minimal, the impact of pore water pressure on soil strength is generally negligible. Consequently, the strength and deformation of the soil are predominantly dictated by the ESSS, meaning that effective stress governs the deformation and strength of the soil.

Therefore, considering solely the contribution of effective stress to shear strength, the shear strength of both saturated and unsaturated soils can be uniformly expressed as

$$\tau_f = c' + [\sigma_t - u_a + S_e(u_a - u_w)]\tan\varphi' \tag{9}$$

where c' is the effective cohesion for both saturated and unsaturated soils, and φ' is the effective internal friction angle for both states. These parameters can be ascertained in the laboratory using triaxial consolidated drained shear tests or direct shear slow shear tests, thereby providing unified shear strength parameters for both saturated and unsaturated soil conditions.

The effective stress equations for saturated and unsaturated soils were combined with the four-parameter Van Genuchten model to predict the shear strengths of four different types of unsaturated soils, namely, expansive soils, pulverized clays, clayey sandy soils, and grey clayey soils, respectively (Shao *et al*. 2018a). The results show that the theoretical predictions agree well with the test values within the range of test accuracy, thus verifying the applicability of the equation in testing and engineering.

4. An EBM theoretical system considering effective stress in unsaturated soils

Numerous factors can induce slope sliding, yet the fundamental cause of landslides is the existence of a sliding surface within the rock and soil mass. The shear stress on this surface attains the shear strength of the soil, thereby undermining the stability of that section of the rock and soil mass. In the absence of pore fluid pressure, the shear strength of the soil is dictated by effective stress. Hence, slope stability analysis predicated on effective stress possesses a sound theoretical foundation.

The Bishop method, introduced by Bishop in 1955, is one of the most extensively employed limit equilibrium methods in slope stability analysis. It models the sliding soil mass as a rigid body rotating around a center and calculates the sliding and resisting forces using the method of slices, ultimately deriving the stability safety factor while accounting for the interaction forces between soil slices. The TBM assumes that the pore water pressure on the sliding surface is zero or positive, thus disregarding the effect of matric suction when the sliding surface lies within an unsaturated zone. Although some researchers have sought to incorporate matric suction into the TBM, there remains a paucity of systematic theoretical analysis and discussion concerning the calculation and implementation of unsaturated effective stress in the Bishop method.

Building on this foundation, this paper proposes an EBM that accounts for effective stress in unsaturated soils. This method employs a unified effective stress equation and shear strength theory applicable to both saturated and unsaturated soils, possessing clear physical significance.

A simple unsaturated slope is used to illustrate the calculation method of the FOS using the EBM. Fig. 5 shows the force diagram of a simple unsaturated slope using the Bishop method. In the case where only the effective stress contribution to the shear strength is considered, according to the static equilibrium condition it can be obtained that

$$\begin{cases} T_i' = \dfrac{c_i' L_i + \left(N_i - u_a L_i + S_e(u_a - u_w)L_i\right)\tan\varphi_i'}{F_S} \\ N_i = \dfrac{1}{m_{ai}}\left[W_i + Y_i + \Delta H_i - \dfrac{\left[c_i' - \left(u_a - S_e(u_a - u_w)\right)\tan\varphi'\right]L_i \sin\alpha_i}{F_S}\right] \\ m_{ai} = \cos\alpha_i + \dfrac{\sin\alpha_i \tan\varphi'}{F_S} \\ W_i + Y_i + \Delta H_i = N_i\cos\alpha_i + T_i\sin\alpha_i \end{cases} \tag{10}$$

where T_i' is the effective shear strength at the bottom surface of the soil strip; N_i is the total normal force at the bottom surface of the soil strip; and N_i' is the effective normal force at the bottom surface of the soil strip ($N_i' = N_i - u_a L_i + S_e(u_a - u_w)L_i$). W_i is the weight of the i-th soil strip ($W_i = \gamma h_{1i} + \gamma_m h_{2i}$); γ is the natural unit weight of the soil in the unsaturated zone; γ_m is the saturated unit weight of the soil in the saturated zone; h_{1i} is the height of the soil strip above the phreatic line; h_{2i} is the height of the soil strip below the phreatic line; Y_i is the vertical seismic inertial force of the i-th soil strip; ΔH_i is the resultant tangential force on the side of the i-th soil strip ($\Delta H_i = H_{i+1} - H_i$).

According to the overall moment equilibrium condition of the entire sliding soil mass, the sum of the moments of the forces acting on each soil strip about the center of the circle is zero. Since the inter-strip forces P_i and H_i appear in pairs, are equal in magnitude, and opposite in direction, the inter-strip forces of the entire sliding soil mass do not produce a moment about the center. The normal stress N_i on the sliding surface also passes through the center, thus not producing a moment. Therefore, only the weight W_i and the tangential force T_i on the sliding surface produce moments about the center. When considering seismic inertial forces, both horizontal and vertical seismic inertial forces also produce moments about the center. Thus, the moment equilibrium equation is

$$\sum\left(W_i + Y_i\right)R\sin\alpha_i + \sum X_i R\cos\alpha_i = \sum \frac{c_i' L_i + \left(N_i - u_a L_i + S_e(u_a - u_w)L_i\right)\tan\varphi_i'}{F_S} R \tag{11}$$

where R is the radius of the sliding arc; X_i is the horizontal seismic inertial force of the i-th soil strip. The FOS can be expressed as

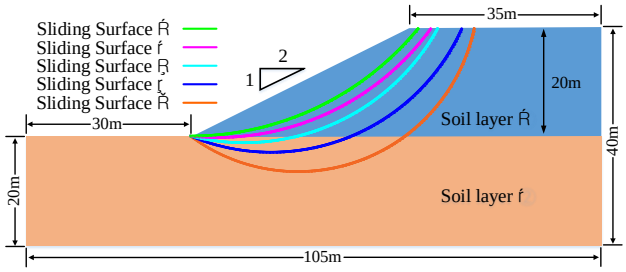

Fig. 6 Simple Saturated Soil Slope

$$F_S = \frac{\sum \frac{1}{m_{ai}}\left[c_i' B_i + \left(W_i + Y_i + \Delta H_i\right)\right]\tan\varphi'}{\sum\left(W_i + Y_i\right)\sin\alpha_i + \sum X_i\sin\alpha_i} + \frac{\sum \frac{1}{m_{ai}}\left[\left[u_a - S_e(u_a - u_w)\right]\left(m_{ai} - \cos\alpha_i\right)L_i\right]\tan\varphi'}{\sum\left(W_i + Y_i\right)\sin\alpha_i + \sum X_i\sin\alpha_i} - \frac{\sum\left[\left[u_a L_i - S_e(u_a - u_w)L_i\right]\tan\varphi'\right]}{\sum\left(W_i + Y_i\right)\sin\alpha_i + \sum X_i\sin\alpha_i} \tag{12}$$

Eq. (12) is the calculation formula for the FOS of the EBM based on the unified effective stress equation for saturated and unsaturated conditions. In the Bishop method, the tangential force between soil strips is not considered and is assumed to be zero.

A computational analysis program is written using computer programming languages to calculate the FOS of the EBM. First, the search range for the center of the sliding surface and the entry and exit range of the arc are input. Within the search range, a sliding surface is selected, and the EBM calculation program is used to solve Eq. (12). Since the term m_{ai} on the right side of the equality in Eq. (12) includes the FOS(F_s), it must be determined through iterative calculations. Initially, F_s is set to 1, m_{ai} is calculated, and then F_s is solved using Eq. (12). This iteration continues until convergence is achieved. The most critical sliding surface is determined through continuous search and calculation.

5. Verification of the accuracy of the EBM calculation program

In both the EBM and the TBM, the calculation of effective stress in the saturated zone is based on Terzaghi's effective stress equation. For saturated soil slopes, the FOS calculation formulas of the two methods are the same, differing only in their computational procedures. The differences lie in the search method for the sliding surface and the calculation step size. Based on this, the stability of saturated soil slopes is analyzed using both the EBM and the TBM to verify the accuracy of the EBM calculation program.

Fig. 6 shows a simple saturated soil slope with a dam height of 20 m and a slope ratio of 1:2. This slope consists of two soil layers: soil layer ① has a saturated unit weight of 19.5 N/m³, and soil layer ② has a saturated unit weight

Table 1 Calculation Results of the FOS for Saturated Slope Sliding

Sliding surface	EBM	TBM	Relative error
Sliding surface ①	1.136	1.165	-2.49%
Sliding surface ②	1.160	1.151	+0.78%
Sliding surface ③	1.200	1.173	+2.30%
Sliding surface ④	1.300	1.305	-0.38%
Sliding surface ⑤	1.470	1.514	-2.91%

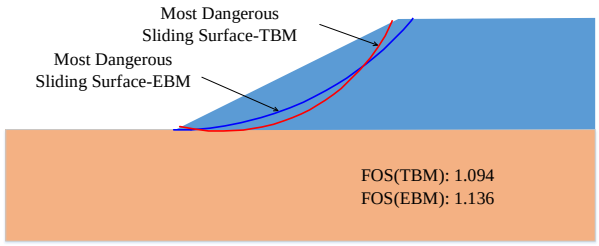

Fig. 7 The Most Critical Sliding Surfaces Searched by the Two Methods

of 20.6 N/m³. The effective internal friction angle and effective cohesion of soil layer ① are 31.3° and 13.2 kPa, respectively, while those of soil layer ② are 30.4° and 12 kPa.

It is generally assumed that the phreatic line in a saturated slope follows the surface of the slope, meaning the slope surface is a zero water pressure surface. Therefore, for this simple saturated soil slope, the pore water pressure at various points along the slope can be calculated using Eq. (2) based on the height of the phreatic line (slope surface). Based on the inclination of the phreatic line, the maximum calculation error of the pore water pressure at the slope location can be determined to be 20% using Eq. (3).

Based on the pore water pressure calculation results, the effective stress at various points in the saturated zone can be determined. Stability analysis of the saturated soil slope is then performed using both the EBM and the TBM. First, the most critical sliding surface of the slope is searched for and its FOS calculated using the EBM proposed in this paper. The most critical sliding surface is sliding surface ① in Fig. 6, with a FOS of 1.136. Under the same soil layer parameters and phreatic line, the TBM built into the SLOPE/W program is used to calculate the FOS for sliding along sliding surface ①, which is 1.165. The relative error in the FOS between the two methods is 2.49%.

Since the most critical sliding surface searched by the EBM calculation program is relatively shallow, to comprehensively consider the reliability of the FOS results of the EBM, four deeper sliding surfaces (as shown in Fig. 6 as sliding surfaces ② to ⑤) are selected. The results are shown in Table 1.

As shown in Table 1, for five sliding surfaces at different depths, the relative error of the FOS calculated by the EBM and the TBM is within 3%. This error arises because, in the SLOPE/W program, the fixed sliding surface is achieved by setting several control points, and the FOS calculation divides the soil into strips between adjacent control points, differing from the strip division by step size in the EBM. Overall, for the same sliding surface, the relative error of the FOS calculated by the EBM is smaller compared to the TBM, and it is within the calculation error range.

Additionally, to verify the reliability of the most critical sliding surface search results of the EBM calculation program, the TBM is used to calculate the most critical sliding surface and its FOS for the simple saturated soil slope, and the results are compared with those of the EBM. The calculation results of the most critical sliding surface are shown in Fig. 7. The FOS for the most critical sliding surface calculated by the EBM and the TBM are 1.136 and 1.094, respectively, with a relative error of about 3.7%.

In many engineering fields, a relative error of 3.7% is typically deemed acceptable. For instance, in slope stability analysis, the typical range of critical FOS is between 1.15 and 1.30, which sufficiently accounts for uncertainties and minor deviations in calculations.

As illustrated in Fig. 7, the depth of the most critical sliding surface determined by the EBM is marginally less than that calculated by the TBM. The exit locations of the most critical arcs identified by the two methods are nearly identical, exhibiting an entry range discrepancy of approximately 3 meters.

Calculation errors in the most critical slip surface and FOS primarily result from the EBM performing slope stability analysis with the phreatic line as the input condition, where both pore water pressure in the saturated zone and matric suction in the unsaturated zone are directly determined based on the phreatic line. Due to the assumptions inherent in the calculation method, there is some error in the saturated zone's pore water pressure, which is also related to the angle of the phreatic line: the flatter the phreatic line, the smaller the calculation error of the pore water pressure. In practical geotechnical engineering, the phreatic line is generally quite flat. For slopes with a phreatic line angle of less than 20°, the proposed stability analysis method provides relatively accurate results, fully meeting engineering precision requirements. While simplifying the calculation process, EBM ensures sufficient computational accuracy and retains significant engineering application value.

6. Analysis of the influence of unsaturated effective stress on slope stability

Currently, most geotechnical structures are unsaturated for long periods of time (Bella 2021), and changes in groundwater have a large impact on the stability of geotechnical structures (Amornfa *et al.* 2023, Lim *et al.* 2023, Park *et al.* 2019). Most reported slope failures have occurred in these unsaturated regions. Variations in the unsaturated state detrimentally impact slope stability. On this basis, the specific implementation steps of EBM considering unsaturated effective stress based on the case of known phreatic line are given, and the influence of unsaturated effective stress on slope stability is analyzed.

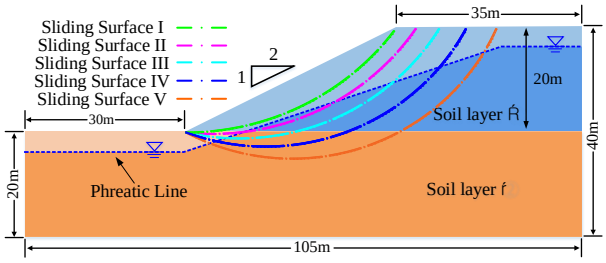

Fig. 8 Simple Unsaturated Soil Slope

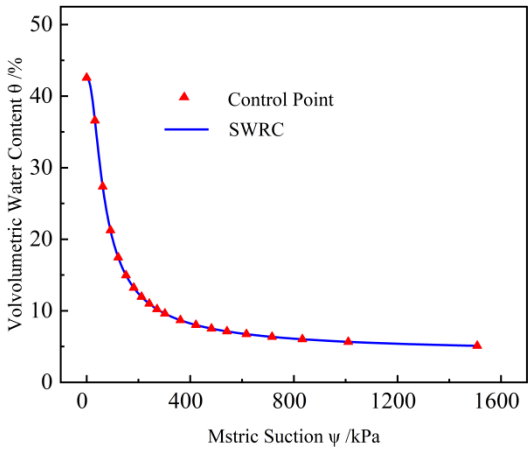

Fig. 9 soil-water characteristic curves

For the saturated soil slope in Fig. 6, under prolonged infiltration and drying conditions, the phreatic line will drop, and the saturated slope will become an unsaturated slope until the phreatic line stabilizes, as shown in Fig. 8. The natural unit weight and saturated unit weight of soil layer ① are 18.1 N/m³ and 19.5 N/m³, respectively. The natural unit weight and saturated unit weight of soil layer ② are 19.3 N/m³ and 20.6 N/m³, respectively. When using the EBM for calculation, the natural unit weight is used for the unsaturated zone, and the saturated unit weight is used for the saturated zone. When the effect of pore water pressure on shear strength is not considered, shear strength is controlled solely by effective stress. Therefore, the shear strength parameters of saturated and unsaturated soils remain consistent. The shear strength parameters of soil layers ① and ② use the effective internal friction angle and effective cohesion of the saturated soil slope.

In open strata, the pore air pressure u_a is 0, and the matric suction in the unsaturated zone is the negative pore water pressure. Based on the height of the phreatic line, the pore water pressure in the saturated and unsaturated zones is calculated using Eq. (2). Based on the inclination of the phreatic line, the maximum calculation error of pore water pressure at the slope surface location is estimated to be 10% using Eq. (3). The effective stress at any point in the saturated and unsaturated zones is calculated using the unified effective stress result from Eq. (6), where the effective saturation S_e in the saturated zone is 1. The effective saturation of the unsaturated zone soil is determined through the soil-water characteristic curve. The specific method is to input several points of the soil-water characteristic curve into the calculation program in this paper, and use the interpolation function to determine the effective saturation corresponding to different matric suctions in the unsaturated zone. The soil-water characteristic curves of the soil layers of the simple unsaturated soil slope are shown in Fig. 9.

Table 2 Calculation Results of FOS for Unsaturated Slopes

Sliding surface	Consider unsaturated	Don't consider unsaturated	Improvement (FOS)
Sliding surface I	1.750	1.710	+2.34%
Sliding surface II	1.697	1.680	+1.01%
Sliding surface III	1.800	1.730	+4.05%
Sliding surface IV	2.050	1.830	+12.02%
Sliding surface V	2.350	1.950	+20.51%

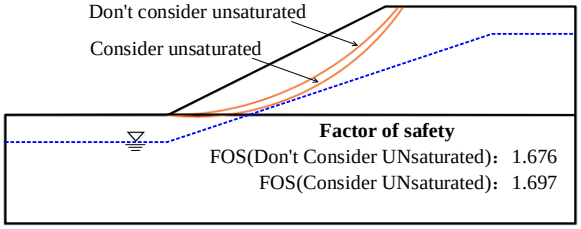

Fig. 10 Calculation Results of the Most Critical Sliding Surface

Based on the aforementioned unsaturated parameters and considering the effective stress in the unsaturated zone, the EBM is employed to calculate the most critical arc and FOS for the unsaturated slope. These results are compared with those obtained without considering the unsaturated condition to analyze the impact of matric suction on slope stability.

By specifying the search range for the circle center along with the entry and exit points, the EBM, which accounts for the effective stress in the unsaturated zone, is employed to identify the most critical sliding surface. The most critical sliding surface is shown as surface II in Fig. 8, located in the unsaturated zone. Five different sliding surfaces (including the most critical sliding surface found by the EBM considering unsaturated effective stress) are selected as shown in Fig. 8, with sliding surfaces I and II located in the unsaturated zone. For the five selected sliding surfaces, the FOS are calculated using the EBM, both accounting for and not accounting for unsaturated effective stress. The results are presented in Table 2.

As illustrated in Table 2, for sliding surfaces I to V, the FOS calculated with consideration of the effective stress in the unsaturated zone are consistently higher than those calculated without it, showing an increase ranging from 1.01% to 20.51%.

The EBM, based on the unified effective stress theory for both saturated and unsaturated conditions, incorporates the matric suction in the unsaturated zone above the phreatic line into the calculation framework, thereby more accurately representing the stress state in the unsaturated zone. On this basis, a comprehensive analysis of slope stability was conducted by integrating the unified shear

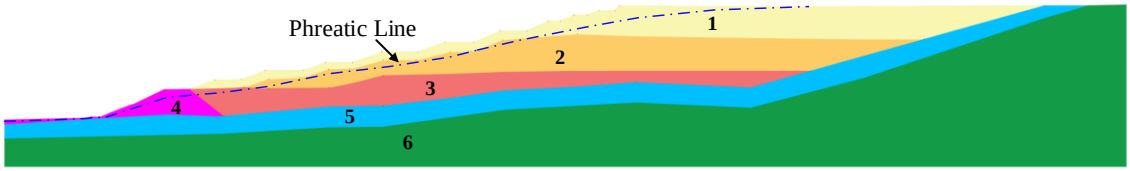

Fig. 11 Two-dimensional calculation profile of tailings dam

Table 3 Physical parameters of soil layer

Number	Material type	γ_{unsat} (kN/m^3)	γ_{sat} (kN/m^3)	Shear strength parameters	
				c (kPa)	*φ*(°)
1	Tail silt①	16.9	18.7	5	26.3
2	Tail silt②	18.8	19.3	6	27.5
3	Tail silt③	19.0	19.6	8	28.9
4	Plain fill	20.0	20.6	4	35.5
5	Heavily weathered granite	26.5	27.0	155	34.0
6	Moderately weathered granite	27.0	27.3	170	39.0

strength criterion for both saturated and unsaturated soils. This method precisely quantifies the contribution of matric suction to shear strength, significantly enhancing the reliability of slope stability assessment. The results indicate that, compared to traditional methods, the FOS for slope stability considering unsaturated effective stress is increased by up to 20.51%, a significant improvement with important engineering application value.

Additionally, the most critical sliding surface of the slope is identified, and its FOS is calculated without considering unsaturated effective stress, to analyze the impact of including unsaturated effective stress on the location of the critical sliding surface. As illustrated in Fig. 10.

According to Fig. 10, the most critical sliding surfaces identified, whether considering the unsaturated effective stress or not, are both situated in the unsaturated zone. The critical sliding surface calculated with unsaturated effective stress is deeper and exhibits a higher FOS. Therefore, accurately accounting for the stress and strength in the unsaturated zone positively influences slope stability.

Overall, matric suction positively influences slope stability, consistent with established principles. Accounting for unsaturated conditions enables a more precise determination of the most critical sliding surface and FOS, which is crucial for engineering design and safety evaluation.

7. Engineering application

A tailings dam is a structure built to intercept a valley or enclose an area for storing tailings. In the event of a dam failure, it would pose a serious threat to human life and property. Therefore, timely assessment of the dam's stability is crucial. As a typical unsaturated slope, the stability analysis of a tailings dam must account for the influence of unsaturated effective stress, a key factor in accurately assessing the dam's slope stability.

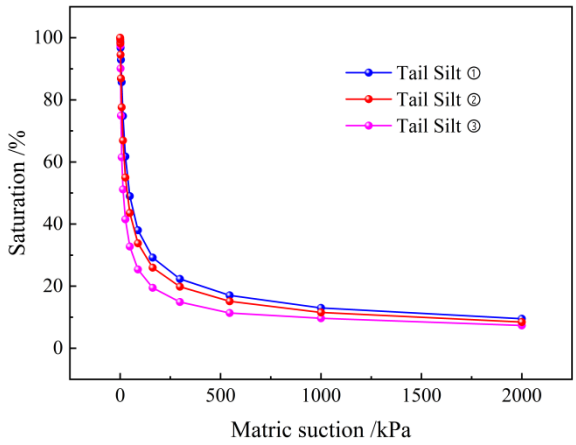

Fig. 12 soil-water characteristic curve of tail silt

This paper demonstrates the application of the EBM in practical engineering, using a specific tailings dam project as an example. The tailings embankment dam was constructed using the upstream method, with an existing elevation of 236 m, a total dam height of 116 m, and a maximum height of 28 m for the initial dam. A typical two-dimensional cross-section of the tailings dam was chosen for stability analysis. The division of the dam's soil layers and the measured phreatic line are shown in Fig. 11, with the physical parameters of the dam materials detailed in Table 3.

First, the boundaries of each soil layer in the tailings dam were input into the EBM calculation program to create a two-dimensional model. Next, the measured phreatic line data was imported into the program as control point coordinates. The measured phreatic line of the tailings dam has an average angle of approximately 10° at the embankment slope. Based on this, the maximum relative error of the pore pressure, determined using an approximate calculation method, is about 3%, meeting the engineering accuracy requirements.

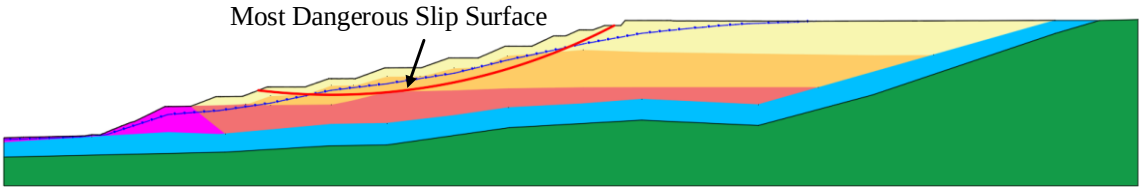

Fig. 13 Stability calculation results of tailings dam

The soil-water characteristic curve (SWCC) for the dam material (Tail silt) is shown in Fig. 12. Based on these conditions, the EBM was used to determine the most dangerous slip surface and FOS at the embankment location of the tailings dam.

Under the measured phreatic line condition, the most dangerous slip surface of the dam, calculated using the EBM and accounting for unsaturated effective stress, is shown in Fig. 13, with a FOS of 2.80. The most dangerous slip surface lies within the tail silt layer, crosses the phreatic line, and encompasses both the unsaturated and saturated zones. This result highlights the importance of accurately considering unsaturated effective stress in the stability analysis of the tailings dam slope.

As technology advances and safety demands grow, water level monitoring systems have become a standard feature in various slope engineering projects, significantly improving the accuracy of phreatic line measurements. For stability analysis of geotechnical engineering slopes (such as earth dams, embankments, natural slopes, and tailings dams), calculations can be directly based on measured phreatic lines. The EBM proposed in this paper, which is based on measured phreatic lines and considers the unsaturated effective stress field, makes slope stability analysis faster, simpler, and more accurate, providing significant theoretical support and practical value for the design optimization and safety assessment of slope engineering.

8. Conclusions

(1) Building on the unified effective stress equation for both saturated and unsaturated soils, this paper proposes an EBM that incorporates the effective stress of unsaturated soils. It examines the methodology for determining pore water pressure using the phreatic line and analyzes the correlation between pore water pressure calculation errors and the inclination angle of the phreatic line.

(2) The stability of a simple saturated soil slope was evaluated using both the EBM and the TBM. For the same sliding surface, the relative error in the FOS was found to be within 3%. For the most dangerous slip surface, the slide-out position is almost identical, with the slide-in range differing by only 3m. The relative error in the FOS is approximately 3.7%, which is sufficient to meet engineering requirements. Overall, under identical conditions, the results of the EBM and the TBM in identifying the most critical sliding surface and calculating the FOS were remarkably similar, thereby verifying the reliability of the EBM computational procedure.

(3) Using an unsaturated slope as an example, this analysis examines the impact of unsaturated zone effective stress on slope stability. The results indicate that for the same sliding surface, the FOS increased by 1.01% to 20.51% when incorporating effective stress in the unsaturated zone. Furthermore, compared to the most critical sliding surface calculated without considering unsaturated effective stress, the critical sliding surface identified with unsaturated effective stress is deeper and exhibits a higher FOS. Accounting for unsaturated effective stress exerts a beneficial influence on slope stability and holds significant importance for engineering design and safety evaluation.

(4) The EBM, based on the unified effective stress theory for both saturated and unsaturated conditions, incorporates matric suction in the unsaturated zone above the phreatic line into the calculation framework, more accurately representing the stress state in this zone. A comprehensive slope stability analysis was conducted by integrating the unified shear strength criterion for both saturated and unsaturated soils. This method precisely quantifies the contribution of matric suction to shear strength, significantly improving the reliability of slope stability assessments. These enhancements lead to a notable improvement in the Factor of Safety (FOS) for slope stability when considering unsaturated effective stress, compared to traditional methods.

(5) This paper uses a simple slope as an example to verify the reliability and advantages of the EBM and applies it to a practical tailings dam project. The method is applicable to various geotechnical slopes, including earth dams, embankments, and natural slopes, and offers significant value for the design optimization and safety assessment of slope engineering. However, the application of this method in complex geotechnical slope engineering projects, as well as its ability to analyze slope stability under seismic conditions, remains an area for further research.

Acknowledgements

This work is supported by the National Natural Science Foundation of China (No. 52079018), International Cooperation Fund Project of DUT-BSU Joint Institute(No. 2305).

References

Alencar, A., Galindo, R. and Melentijevic, S. (2021), "Influence of the groundwater level on the bearing capacity of shallow foundations on the rock mass", *Bull Eng Geol. Environ.*, **80**, 6769-6779. https://doi.org/10.1007/s10064-021-02368-2.

Amornfa, K., Quang, H.T. and Tuan, T.V. (2023), "Effect of groundwater level change on piled raft foundation in Ho Chi Minh City, Viet Nam using 3D-FEM", *Geomech. Eng.*, **32**(4), 387-396. https://doi.org/10.12989/gae.2023.32.4.387.

Bella, G. (2021), "Water retention behaviour of tailings in unsaturated conditions", *Geomech. Eng.*, **26**(2), 117-132. https://doi.org/10.12989/gae.2021.26.2.117.

Bishop, A.W. (1955), "The use of the slip circle in the stability analysis of slopes", *Géotechnique*, **5**(1), 7–17. https://doi.org/10.1680/geot.1955.5.1.7.

Bishop, A.W. (1959), "The principle of effective stress", *Teknisk Ukeblad*, **39**, 859-863.

Bishop, A.W. and Blight, G.E. (1963), "Some aspects of effective stress in saturated and partly saturated soils", *Géotechnique*, **13**(3), 177-197. https://doi.org/10.1680/geot.1963.13.3.177

Cheng, H., Wu, Z.J., Chen, H. and Zhou, X. (2024), "Stability analysis of unsaturated–saturated soil slopes under rainfall infiltration using the rigorous limit equilibrium method", *Bull. Eng. Geol. Environ.*, **83**, 147. https://doi.org/10.1007/s10064-024-03623-y

Cheng, Y.M., Lansivaara, T. and Wei, W.B. (2007), "Two-dimensional slope stability analysis by limit equilibrium and strength reduction methods", *Comput. Geotech.*, **34**(3), 137-150. https://doi.org/10.1016/j.compgeo.2006.10.011.

De Boer, R. and Ehlers, W. (1990), "The development of the concept of effective stresses", *Acta Mechanica*, **83**(1-2), 77-92. https://doi.org/10.1007/BF01174734.

Deng, D.P., Lu, K. and Li, L. (2019), "LE analysis on unsaturated slope stability with introduction of nonlinearity of soil strength", *Geomech. Eng.*, **19**(2), 179-191. https://doi.org/10.12989/gae.2019.19.2.179.

Fredlund, D.G. (2006), "Unsaturated soil mechanics in engineering practice", *J. Geotech. Geoenviron. Eng.*, **132**(3), 286-321. https://doi.org/10.1061/(ASCE)1090-0241(2006)132:3(286).

Fredlund, D.G., Morgenstern, N.R. and Widger, R.A. (1978), "The shear strength of unsaturated soils", *Can. Geotech. J.*, **15**(3), 313-321. https:// doi.org/10.1139/t78-029.

Garakani, A.A., Sadeghi, H., Saheb, S. and Lamei, A. (2020), "Bearing capacity of shallow foundations on unsaturated soils: analytical approach with 3D numerical simulations and experimental validations", *Int. J. Geomech.*, **20**(3), 04019181. https://doi.org/10.1061/(ASCE)GM.1943-5622.0001589.

Gudehus, G. (2021), "Implications of the principle of effective stress", *Acta Geotechnica*, **16**, 1939-1947. https://doi.org/10.1007/s11440-020-01068-7.

Hu, Y.N., Ding, Y. and Sun, Z.B. (2021), "An efficient approach for stability analysis of rock slopes subjected to a transient drawdown", *Geomech. Eng.*, **27**(4), 405-417. https://doi.org/10.12989/gae.2021.27.4.405.

Hua, C.Y., Yao, L.Y., Song, C.G. and Ni, Q. (2022), "Variational method for determining slope instability based on the strength reduction method", *Bull. Eng. Geol. Environ.*, **81**, 395. https://doi.org/10.1007/s10064-022-02895-6.

Jennings, J.E.B. and Burland, J.B. (1962), "Limitations to the use of effective stresses in partly saturated soils", *Géotechnique*, **12**(2), 125-144. https://doi.org/10.1680/geot.1962.12.2.125.

Khalili, N. and Khabbaz, M.H. (1998), "A unique relationship for χ for the determination of the shear strength of unsaturated soils", *Géotechnique*, **48**(5), 681-687. https://doi.org/10.1680/geot.1998.48.5.681

Khalili, N., Geiser, F. and Blight, G.E. (2004), "Effective stress in unsaturated soils: review with new evidence", *Geomechanics*, **4**(2), 115-126. https://doi.org/10.1061/(ASCE)1532-3641(2004)4:2(115).

Li, Y.L., Yao, A.J., Li, H., Gong, T. and Tian, T. (2023), "Calculation method of multi-stage earth pressure for foundation excavation considering excavation process", *Acta Geotechnica*, **18**, 6123-6141. https://doi.org/10.1007/s11440-023-02037-6.

Lim, H., Park, J., Kim, J. and Ko, J. (2023), "Numerical study on stability and deformation of retaining wall according to groundwater drawdown", *Geomech. Eng.*, **33**(2), 195-202. https://doi.org/10.12989/gae.2023.33.2.195.

Liu, S.Y., Shao, L.T. and LI, H. (2015), "Slope stability analysis using the limit equilibrium method and two finite element methods", *Comput. Geotech.*, **63**, 291-298. https://doi.org/10.1016/j.compgeo.2014.10.008

Lu, N., Godt, J.W. and Wu, D.T. (2010), "A closed-form equation for effective stress in unsaturated soil", *Water Resour Res.*, **46**(5), 1-14. https://doi.org/10.1029/2009WR008646.

Lu, N., Wayllace, A. and Oh, S. (2013), "Infiltration-induced seasonally reactivated instability of a highway embankment near the Eisenhower Tunnel Colorado USA", *Eng. Geol.*, **162**, 22-32. https://doi.org/10.1016/j.enggeo.2013.05.002.

Morgenstern, N.R. and Price, V.E. (1965), "The analysis of the stability of general slip surfaces", *Géotechnique*, **15**(1), 79-93. https://doi.org/10.1680/geot.1965.15.1.79.

Oh, S. and Lu, N. (2015), "Slope stability analysis under unsaturated conditions: case studies of rainfall-induced failure of cut slopes", *Eng. Geol.*, **184**, 96-103. https://doi.org/10.1016/j.enggeo.2014.11.007.

Park, D., Kim, I.; Kim, G. and Lee, J. (2019), "Effect of groundwater fluctuation on load carrying performance of shallow foundation", *Geomech. Eng.*, **18**(6), 575-584. https://doi.org/10.12989/gae.2019.18.6.575.

Pirjalili, A., Garakani, A.A., Golshani, A. and Mirzaii, A. (2020), "A suction controlled ring device to measure the coefficient of lateral soil pressure in unsaturated soils", *Geotech. Test. J.*, **43**(6), 1379-1396. https://doi.org/10.1520/GTJ20190099.

Shao, L.T. and Guo, X.X. (2014a), "New explanation of the effective stress", Beijing: China Waterpower Press.

Shao, L.T., Guo, X.X. and Zhao, B.Y. (2018c), "On effective stress and effective stress equation", *Proceedings of the China-Europe Conference on Geotechnical Engineering*, Springer, Cham. https://doi.org/10.1007/978-3-319-97112-4_15.

Shao, L.T., Guo, X.X. and Zheng, G.F. (2015), "Intergranular stress, soil skeleton stress and effective stress", *Chinese J. Geotech. Eng.*, **37**(8), 1478-1483. (in Chinese).

Shao, L.T., Guo, X.X., Liu, S.Y., *et al.* (2018b), "Effective stress and equilibrium equation for soil mechanics", Leiden: CRC Press. https://doi.org/10.1201/9781315107554.

Shao, L.T., Liu, G. and Guo, X.X. (2013), "Uniform effective stress equation for soil mechanics", (Ed., Delage P.), *Proceedings of the 18th ICSMGE*, Paris: Presses des ponts.

Shao, L.T., Qin, Y.L., Guo, X.X., et al. (2018a), "The validation of the effective stress principle of unsaturated soils", *Chinese J. Undergr. Sp. Eng.*, **14**(6), 1476-1483. (in Chinese).

Shao, L.T., Zheng, G.F., Guo, X.X. and Liu, G.. (2014b), "Principle of effective stress for unsaturated soils", *Unsaturated Soils: Res. Appl.*, 239-245. https://doi.org/10.1201/b17034-32.

Shin, H. (2023), "Static and quasi-static slope stability analyses using the limit equilibrium method for mountainous area", *Geomech. Eng.*, **34**(2), 187-195. https://doi.org/10.12989/gae.2023.34.2.187.

Sivakumar Babu, G.L. and Murthy, D.S. (2005), "Reliability analysis of unsaturated soil slopes", *J. Geotech. Geoenviron. Eng.*, **131**(11), 1423-1428. https://doi.org/10.1061/(ASCE)1090-

0241(2005)131:11(1423).
Skempton, A.W. (1960), "The pore-pressure coefficient in saturated soils", *Géotechnique*, **10**(4), 186-187. https://doi.org/10.1680/geot.1960.10.4.186.
Skempton, A.W. (1961), "Effective stress in soils, concrete and rocks", *Proceedings of the Conference on Pore Pressure and Suction in Soils*, Butterworths, London.
Song, Y.S., Chae, B.G. and Lee, J. (2016), "A method for evaluating the stability of an unsaturated slope in natural terrain during rainfall", *Eng. Geol.*, **210**, 84-92. https://doi.org/10.1016/j.enggeo.2016.06.007.
Xu, J.S. and Yang, X.L. (2018), "Three-dimensional stability analysis of slope in unsaturated soils considering strength nonlinearity under water drawdown", *Eng. Geol.*, **237**, 102-115. https://doi.org/10.1016/j.enggeo.2018.02.010.
Xu, J.S., Wang, P.F., Huang, F. and Yang, X. (2021), "Active earth pressure of 3D earth retaining structure subjected to rainfall infiltration", *Eng. Geol.*, **293**, 106294. https://doi.org/10.1016/j.enggeo.2021.106294.
Yates, K. and Russell, A. (2023), "The unsaturated characteristics of natural loess in slopes, New Zealand", *Géotechnique*, **73**(10), 871-884. https://doi.org/10.1680/jgeot.21.00042.
Zhai, Q., Tian, G., Ye, W.M., Rahardjo, H., Dai, G. and Wang, S. (2022), "Evaluation of unsaturated soil slope stability by incorporating soil-water characteristic curve", *Geomech. Eng.*, **28**(6), 637-644. https://doi.org/10.12989/gae.2022.28.6.637.
Zhang, L.L., Fredlund, D.G., Fredlund, M.D. and Wilson, G.W. (2013), "Modeling the unsaturated soil zone in slope stability analysis", *Can. Geotech. J.*, **51**(12), 1384-1398. https://doi.org/10.1139/cgj-2013-0394.
Zhang, L.L., Fredlund, M.D., Fredlund, D.G., Lu, H. and Wilson, G.W. (2015), "The influence of the unsaturated soil zone on 2-D and 3-D slope stability analyses", *Eng. Geol.*, **193**, 374-383. https://doi.org/10.1016/j.enggeo.2015.05. 011.